Title

Inhibition of cathepsin S attenuates myocardial ischemia/reperfusion injury by suppressing inflammation and apoptosis

Journal

Journal of Cellular Physiology, 236(2)

ISSN

0021-9541

Authors

Peng, Ke
Liu, Hong
Yan, Bin
et al.

Publication Date

2021-02-01

DOI

10.1002/jcp.29938

Peer reviewed

Received: 20 February 2020 | Accepted: 2 July 2020

DOI: 10.1002/jcp.29938

ORIGINAL RESEARCH ARTICLE

Journal of Cellular Physiology WILEY

Inhibition of cathepsin S attenuates myocardial ischemia/reperfusion injury by suppressing inflammation and apoptosis

Ke Peng[1] | Hong Liu[2] | Bin Yan[3,4] | Xiao-Wen Meng[1] | Shao-Yong Song[1] | Fu-Hai Ji[1] | Zhengyuan Xia[2,5]

[1]Department of Anesthesiology, First Affiliated Hospital of Soochow University, Suzhou, China

[2]Department of Anesthesiology and Pain Medicine, University of California Davis Health, Sacramento, California

[3]Department of Intervention and Cell Therapy, Peking University Shenzhen Hospital, Shenzhen, China

[4]Department of Computer Science, The University of Hong Kong, Pokfulam, Hong Kong

[5]Department of Anesthesiology, The University of Hong Kong, Pokfulam, Hong Kong

Correspondence

Fu-Hai Ji, Department of Anesthesiology, First Affiliated Hospital of Soochow University, 188 Shizi St, Suzhou 215006, China.
Email: jifuhaisuda@163.com

Zhengyuan Xia, Department of Anesthesiology and Pain Medicine, University of California Davis Health, 4150 V St, Suite 1200, Sacramento, CA 95817.
Email: zhyxia@ucdavis.edu

Funding information

Jiangsu Provincial Medical Youth Talents Program, Grant/Award Number: QNRC2016741; Jiangsu Government Scholarship for Overseas Studies, Grant/Award Number: JS-2018-178; Jiangsu Provincial Medical Innovation Team, Grant/Award Number: CXTDA2017043; Suzhou Key Disease Program, Grant/Award Number: LCZX201603; National Natural Science Foundation of China, Grant/Award Numbers: 81601659, 81671880, 81701098, 81873925

Abstract

Myocardial ischemia/reperfusion (I/R) injury leads to high mortality and morbidity due to the incomplete understanding of the underlying mechanism and the consequent lack of effective therapy. The present study revealed and validated key candidate genes in relation to inflammation and apoptosis pathways underlying myocardial I/R injury. Cathepsin S was identified as the top hub protein based on the protein–protein interaction analysis, and, thus, its role during myocardial I/R injury was further investigated. Myocardial I/R in mice resulted in significantly increased levels of myocardial injury biomarkers (cardiac troponin I, lactic dehydrogenase, and creatinine kinase-MB) and inflammatory cytokines (interleukin-1β [IL-1β], IL-6, and tumor necrosis factor-α), elevated apoptosis rate, and upregulated protein expression of cleaved caspase-8, cleaved caspase-3, and cleaved poly ADP-ribose polymerase. These abovementioned changes were blocked by two different selective cathepsin S inhibitors, LY3000328 or MIV-247. Moreover, Kaplan–Meier survival plot showed that cathepsin S inhibition improved 21-day survival rate following myocardial I/R injury. This study demonstrated that the inhibition of cathepsin S alleviated myocardial I/R-induced injury by suppressing inflammation and apoptosis, which may be used in clinical applications of cardioprotection.

KEYWORDS

apoptosis, cardioprotection, cathepsin S, inflammation, myocardial ischemia/reperfusion injury

1 | INTRODUCTION

The deaths resulted from coronary heart disease (CHD) or myocardial infarction (MI) is mainly attributable to the detrimental effects of myocardial ischemia/reperfusion (I/R) injury, in which the restoration of blood flow paradoxically leads to additional damage to the myocardium (Hausenloy & Yellon, 2013). Myocardial I/R injury is often inevitable, especially in procedures of percutaneous coronary intervention, coronary artery bypass grafting with or without cardiopulmonary bypass, and circulatory arrest. Animal studies have indicated many cardioprotective treatments, but there is still no effective therapeutic strategy for preventing myocardial I/R injury in the clinical settings (Chi et al., 2017; Davidson et al., 2019).

A number of mechanisms have been shown to underline the myocardial I/R injury, including oxidative stress, mitochondrial permeability transition pore opening, intracellular calcium overload, inflammation, apoptosis, autophagy, necroptosis, pyroptosis, and ferroptosis (Lei et al., 2019; Toldo, Mauro, Cutter, & Abbate, 2018; S. Wang et al., 2017; Xia, Li, & Irwin, 2016; T. Zhang et al., 2016). Recent studies showed that pharmacological inhibition of inflammation and apoptosis alleviated I/R-induced myocardial injury in rats or hypoxia/reoxygenation-induced injury in cardiomyocytes (J. Chen et al., 2019; Peng et al., 2020; Yuan et al., 2019; J. J. Zhang, Peng, Zhang, Meng, & Ji, 2017). Given the multiple underlying mechanisms, as well as other types of cells involved, targeting only one mechanism may not produce strong enough protective effects against I/R injury in patients with CHD and MI (Davidson et al., 2019).

In this study, we identified several key candidate genes with enriched inflammation and apoptosis signaling pathways underlying myocardial I/R injury on the transcriptional profile by using a bioinformatic approach. Then, the expression of the key genes was validated on several different gene expression profile datasets and in myocardial I/R mice. Furthermore, the effects of cathepsin S inhibition on inflammation, apoptosis, and mortality following I/R-induced myocardial injury in mice were explored.

2 | MATERIALS AND METHODS

The animal experimental protocol was approved by the Ethics Committee for Animal Experimentation of Soochow University. All procedures were performed in accordance with the Guide for the Care and Use of Laboratory Animals (National Institutes of Health).

2.1 | Study workflow

In Part I (Figure 1a), the gene expression profiles of GSE4105 were obtained from the gene expression omnibus (GEO) database. In GSE4105, rat hearts were harvested after myocardial I/R (ischemia for 30 min followed by reperfusion for 2 and 7 days) or sham (SH) surgery. The differentially expressed genes (DEGs) were identified for three comparisons, respectively: IR2 versus SH2 (I/R rats vs. SH rats on Day 2 of reperfusion), IR7 versus SH7 (I/R rats vs. SH rats on Day 7), and IR7 versus IR2 (I/R rats on Day 7 vs. 2). By using the database for annotation, visualization, and integrated discovery (DAVID) database, gene ontology (GO) enrichment, and Kyoto encyclopedia of genes and genomes (KEGG) pathway were analyzed for the DEGs between the three comparisons, respectively. The common DEGs and KEGG pathways were determined.

In Part II (Figure 1b), protein–protein interaction (PPI) network analysis of common DEGs was performed on the search tool for the retrieval of interacting genes/proteins (STRING) database. Hub proteins with rich connectivity were identified. Then, the highly clustered modules of proteins were searched by using the Cytoscape molecular complex detection (MCODE) algorithm. For the key genes encoding the hub proteins, GO and KEGG analyses were conducted on the g:Profiler database. Three key genes involved in the inflammation and apoptosis pathway were verified in two murine

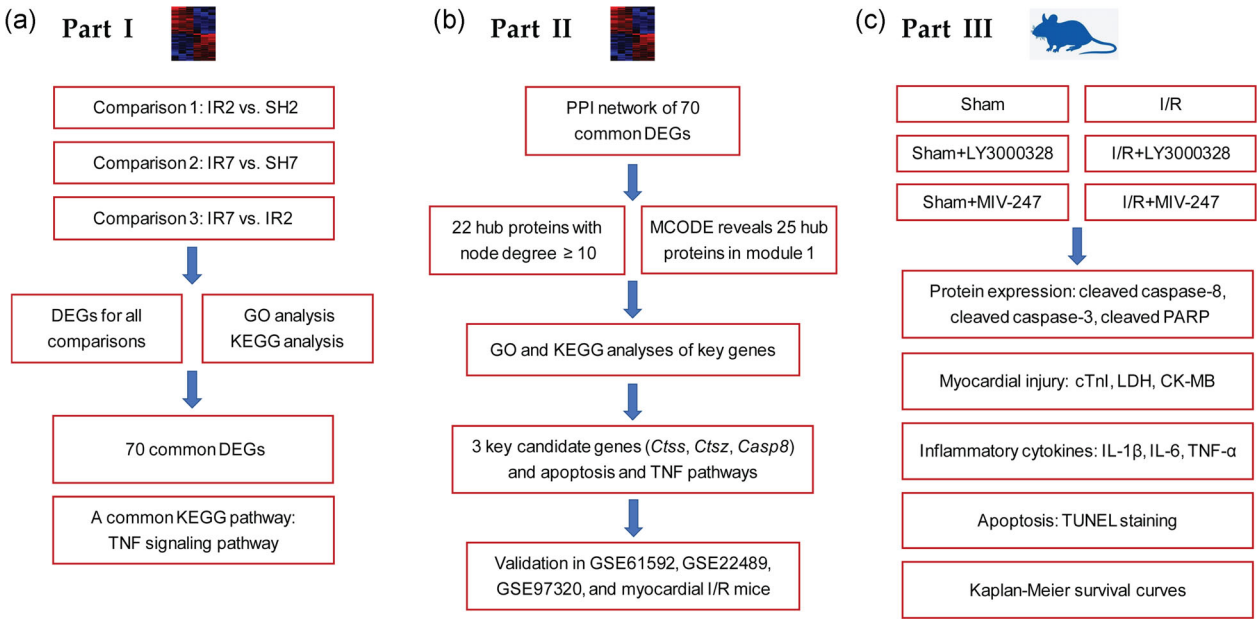

FIGURE 1 Study workflow. (a) Bioinformatic analysis of three comparisons during myocardial I/R injury. (b) Identification of key genes and validation in three datasets and myocardial I/R mice. (c) The effects of cathepsin S inhibition by LY3000328 or MIV-247 on myocardial I/R mice were evaluated. CK-MB, creatinine kinase-MB; cTnI, cardiac troponin I; DEG, differentially expressed gene; GO, gene ontology; IL-1β, interleukin-1β; IL-6, interleukin-6; IR, ischemia/reperfusion; KEGG, kyoto encyclopedia of genes and genomes; LDH, lactic dehydrogenase; MCODE, molecular complex detection; PARP, poly ADP-ribose polymerase; PPI, protein–protein interaction; SH, sham; TNF-α, tumor necrosis factor-α; TUNEL, TdT-mediated dUTP nick-end labeling

datasets (GSE61592 and GSE22489) and one human dataset (GSE97320). Next, the protein expression of the three key genes was determined by western blots in myocardial I/R mice (ischemia of 30 min and reperfusion of 24 hr).

In Part III (Figure 1c), the effects of two different selective cathepsin S (encoded by *ctss* gene) inhibitors, LY3000328 (APExBIO, TX) and MIV-247 (MCE, NJ), on the I/R-induced myocardial injury in mice were tested. An investigator who did not participate in the subsequent studies performed the randomization by using a computer-generated table and prepared the study solutions. Then, mice were randomly assigned to one of six groups: SH, SH + LY3000328, SH + MIV-247, I/R, I/R + LY3000328, and I/R + MIV-247. One of three solutions, LY3000328 (5 mg/kg; Jadhav et al., 2014; Steimle et al., 2016), MIV-247 (200 μmol/kg; Hewitt et al., 2016), or the same volume of vehicle (20% hydroxypropyl-β-cyclodextrin in water), was administered by oral gavage for 3 days, twice daily, starting from 3 days before ischemia. The protein expression of cleaved caspase-8, cleaved caspase-3, and cleaved poly ADP-ribose polymerase (PARP) was determined by western blot. Myocardial injury parameters including serum cardiac troponin I (cTnI), lactic dehydrogenase (LDH), and creatinine kinase-MB (CK-MB) and inflammatory cytokines in the myocardium including interleukin-1β (IL-1β), IL-6, and tumor necrosis factor-α (TNF-α) were tested by using the enzyme-linked immunosorbent assay (ELISA). Myocardial apoptosis was detected by using the TdT-mediated dUTP nick-end labeling (TUNEL) staining. Myocardial I/R-induced mortality at 21 days of reperfusion was assessed with the Kaplan–Meier survival plot.

2.2 | Data acquisition and DEGs identification

After obtaining the gene expression profile of GSE4105 from the GEO database (http://www.ncbi.nlm.nih.gov/geo/), DEGs were identified in IR2 versus SH2, IR7 versus SH7, and IR7 versus IR2, respectively, by using the *limma* package in R language (Ritchie et al., 2015). The criteria for DEGs screening were $p < .05$ and $\log_2|\text{fold change}| > 1$. The gene expression profiles were visualized in volcano plots and heatmaps.

2.3 | GO enrichment, KEGG pathway, and PPI network of DEGs

For the DEGs, GO enrichment of biological process (BP), molecular function (MF), and cellular component (CC) and KEGG pathway analyses were performed on the DAVID database (https://david.ncifcrf.gov/; Jiao et al., 2012). PPI network of 70 common DEGs was conducted on the STRING database (https://string-db.org/; Szklarczyk et al., 2019). To identify highly connected network components, the MCODE algorithm was applied with the Cytoscape software (version 3.7.2, https://cytoscape.org/; Bader & Hogue, 2003; Shannon et al., 2003). For the key genes, functional enrichment and network analyses were conducted on the g:Profiler (https://biit.cs.ut.ee/gprofiler/; Raudvere et al., 2019).

2.4 | Myocardial I/R injury model

Male C57BL/6J mice (8 weeks old) were housed under a controlled condition (12-hr light/dark cycle; 22°C; three mice per cage), with free access to food and water. The myocardial I/R model was established as previously described (T. T. Wang et al., 2019). The mice received intraperitoneal anesthesia with pentobarbital (70 mg/kg). After sternotomy, the left anterior descending coronary artery was temporarily occluded with a reversible snare for 30 min, and then the occlusion was released for blood flow restoration. Myocardial ischemia was confirmed by observing myocardial blanching. The mice were allowed to recover and return to cages. To determine the protein expression of the key genes and the effects of cathepsin S inhibition on myocardial I/R injury at an early stage of reperfusion, the heart samples were harvested after reperfusion for 24 hr.

2.5 | Western blots

The left ventricle tissues were homogenized with lysis buffer containing polymethyl sulfoxide. The proteins were separated using sodium dodecyl sulphate-polyacrylamide gel electrophoresis on 10% gels and transferred to nitrocellulose membranes. Next, the membranes were blocked and incubated at 4°C overnight, with the specific primary antibodies: anti-cathepsin S (1:1,000; ab232740; Abcam), anti-cathepsin Z (1:1,000; ab180580; Abcam), anti-caspase-8 (1:1,000; #4927; Cell Signaling Technology), anti-cleaved caspase-8 (1:1,000; #8592; Cell Signaling Technology), anti-caspase-3 (1:1,000; #9662; Cell Signaling Technology), cleaved PARP (1:500; sc-56196; Santa Cruz Biotechnology), anti-β-tubulin (1:1,000; #15115; Cell Signaling Technology), and anti-GAPDH (1:2,000; AF5009; Beyotime Biotechnology). The membranes were then incubated for 1 hr with horseradish peroxidase-conjugated secondary antibodies. Finally, the blots were visualized with chemiluminescence on the ChemiDoc™ Imaging System (Bio-Rad, Hercules, CA). The images were analyzed by using the Image J software (version 1.44p; National Institutes of Health).

2.6 | Enzyme-linked immunosorbent assay

Serum cTnI, LDH, and CK-MB levels were quantified by using the ELISA kits (Nanjing Jiancheng Bioengineering Research Institute, Nanjing, China). Activities of IL-1β, IL-6, and TNF-α in heart lysates were determined by using the ELISA kits (Multi Sciences, Hangzhou, China). Absorbance values at 450 nm were obtained with a plate reader (MD SpectraMax190; CA) and sample concentrations were determined using a standard curve.

2.7 | TUNEL assay

Myocardial apoptosis was determined by using the TUNEL Detection Kit (Roche, Switzerland). The myocardial slices were counterstained with 4′,6-diamidino-2-phenylindole. Images were captured under a fluorescence microscope (DM2500; Leica Camera, Germany). For each slice, TUNEL-positive nuclei and total myocardial cell nuclei were recorded in four random nonoverlapping fields. The apoptosis rate was then calculated as the ratio of TUNEL-positive cells to all cells.

2.8 | Statistical analysis

The statistical analysis was performed by using the GraphPad Prism software (version 7.0; San Diego, CA). Kolmogorov–Smirnov test was used to check the normality of distribution. Data groups with normal distribution were expressed as mean ± standard deviation and compared with one-way or two-way analysis of variance, followed by Šidàk correction for multiple comparisons. The survival data were depicted by using the Kaplan–Meier plot and were compared by the logrank test. A two-tailed $p < .05$ denoted statistically significant differences.

3 | RESULTS

3.1 | Identification of DEGs in myocardial I/R injury

A total of 10,307 genes were analyzed. There were 353 DEGs in IR2 versus SH2, 447 in IR7 versus SH7, and 340 in IR7 versus IR2 (Figure 2a–c). The numbers of up- and downregulated DEGs for each comparison are shown in Figure 2d. For each comparison, the heatmap shows that the top 50 up- and downregulated DEGs present apparently differential expression profiles (Figure 2e–g). The top 10 up- and downregulated DEGs for each comparison are listed in Table 1. There were 70 common DEGs between IR2 versus SH2 and IR7 versus SH7 (Figure 2h; Table 2).

3.2 | GO and KEGG analyses revealed significantly enriched functional categories and signaling pathways

For IR2 versus SH2, the top 10 enriched BP, CC, and MF terms of DEGs are shown in Figure 3a, with inflammatory response, extracellular exosome, and protein binding among the most enriched terms. For IR7 versus SH7, the top 10 enriched BP, CC, and MF terms

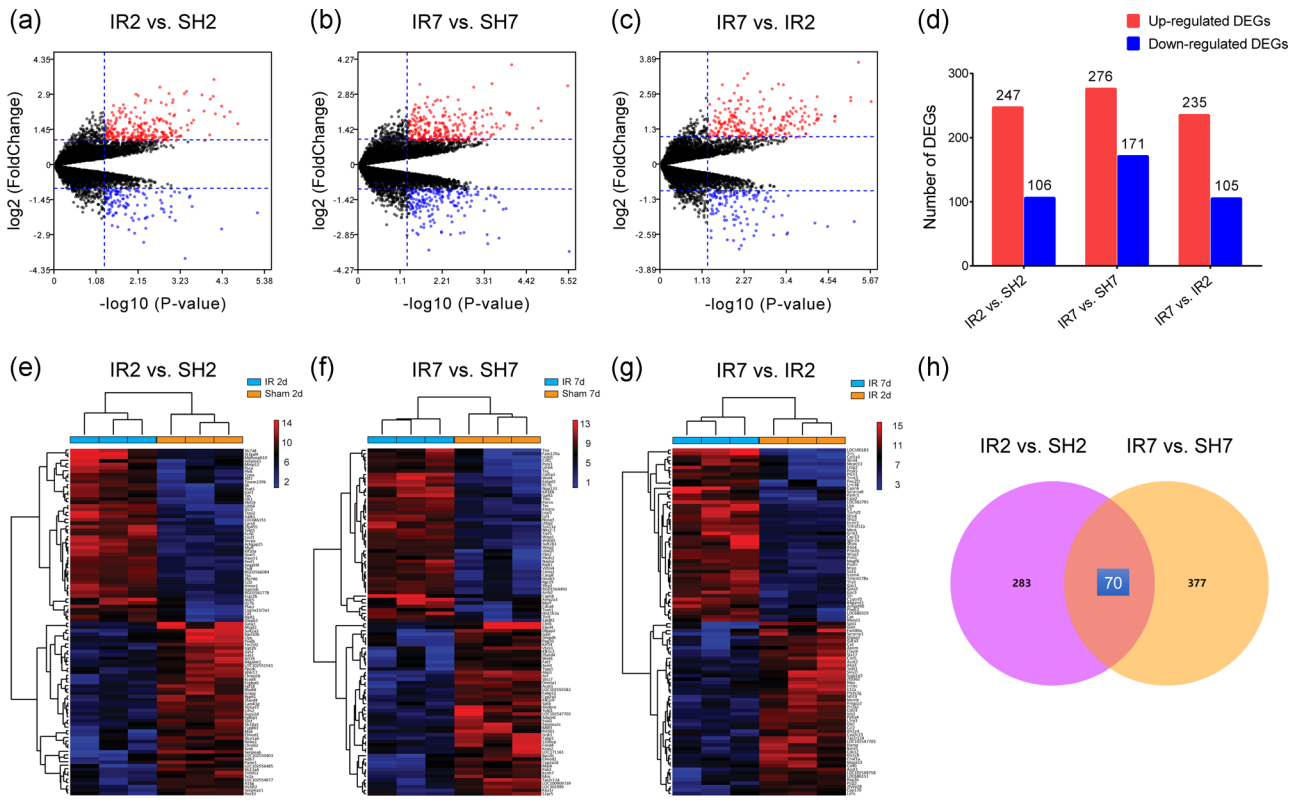

FIGURE 2 Identification of DEGs. (a–c) Volcano plots showing DEGs in IR2 versus SH2, IR7 versus SH7, and IR7 versus IR2, respectively. (d) The numbers of up- and downregulated DEGs. (e–g) Heatmaps of DEGs for three comparisons. (h) Venn's diagram showing 70 common DEGs. DEG, differentially expressed gene; IR, ischemia/reperfusion; SH, sham

TABLE 1 Top 10 up- and downregulated DEGs for each comparison

	Upregulated DEGs	log_2FC	*p*	Downregulated DEGs	log_2FC	*p*
IR2 versus SH2	*Igfbp2*	1.733999	2.11E−05	*Camk1g*	−1.95076	6.64E−06
	Pmf1	2.21911	3.41E−05	*Tm7sf2*	−2.62866	5.55E−05
	Tnik	2.006829	4.60E−05	*Slc6a15*	−1.69824	.00031
	Havcr1	2.45776	5.51E−05	*Rab3a*	−1.24852	.000358
	Angptl4	2.120092	7.93E−05	*Rpl37a*	−1.31331	.000374
	Lilrb4	3.54982	8.50E−05	*Serpina6*	−3.84513	.000462
	Zfp455	2.866917	9.03E−05	*Lnx1*	−1.12897	.000662
	Arhgap25	2.743864	.000108	*Gas1*	−2.27467	.000843
	Srpx2	1.256322	.000113	*B4galnt4*	−1.08918	.00089
	Casp1	1.040423	.00015	*Nudt8*	−1.92285	.001088
IR7 versus SH7	*Entpd1*	3.229013	3.40E−06	*Akp3*	−3.47453	3.02E-06
	Grb10	1.807433	1.67E−05	*Klk1c9*	−1.75985	.000139
	Tfec	2.311825	1.95E−05	*Cyp2a2*	−1.77572	.000168
	Slc22a24	1.524142	2.81E−05	*Grik1*	−2.94961	.000215
	Tmed3	1.647903	6.99E−05	*Fem1b*	−1.48038	.000215
	Matn2	1.503065	7.47E−05	*RGD1565166*	−1.29035	.000263
	Col5a3	4.074292	.000101	*LOC100909684*	−1.23063	.00029
	Nkx2–1	2.134879	.000112	*Slc17a6*	−1.20734	.00036
	Loxl1	2.055356	.000114	*Acr*	−3.17666	.000413
	Lyl1	2.162727	.000131	*Stx17*	−2.80036	.000446
IR7 versus IR2	*Prm1*	2.358962	2.16E−06	*Ppfia4*	−2.07918	6.28E-06
	LOC362795	3.788937	4.81E−06	*Cdkl3*	−2.27638	3.21E-05
	Wisp2	2.368217	7.62E−06	*Ido1*	−2.14717	7.00E-05
	Sfrp2	2.500929	7.75E−06	*Orm1*	−1.11672	.000374
	Mmp2	1.806473	1.97E−05	*Elavl4*	−2.50064	.000394
	Cpt1c	1.807454	2.06E−05	*Mllt3*	−2.56411	.0004
	Srpx2	1.633202	2.12E−05	*Lilrb3*	−1.85464	.000559
	Mmp14	1.863742	4.86E−05	*Mt2A*	−1.34248	.000908
	Cyp1b1	1.720423	5.71E−05	*Klk1c9*	−2.57972	.00092
	Col6a1	1.679621	5.87E−05	*Prl2a1*	−1.89502	.000939

Abbreviations: DEG, differentially expressed gene; FC, fold change; IR, ischemia/reperfusion; SH, sham.

of DEGs are shown in Figure 3b, with proteolysis, extracellular space, and heparin binding among the most enriched terms. For IR7 versus IR2, the top 10 enriched BP, CC, and MF terms of DEGs are shown in Figure 3c, with collagen fibril organization, extracellular space, and heparin binding among the most enriched terms.

The relationship between DEGs and the top five enriched KEGG pathways are depicted in Figure 3d–f. The most significant enriched pathways included the PPAR signaling pathway, phagosome, protein digestion and absorption, phosphatidylinositol-3-kinase–protein kinase B signaling pathway, focal adhesion, and extracellular matrix (ECM)–receptor interaction. Three common KEGG pathways were revealed, including ECM–receptor interaction, amoebiasis, and TNF signaling pathway (Figure 3g).

3.3 | PPI analysis of common DEGs revealed key modules and hub proteins

On the basis of 70 common DEGs, PPI network showed the interactions among the proteins (Figure 4a). A total of 22 hub proteins

TABLE 2 Seventy common DEGs between IR2 versus SH2 and IR7 versus SH7

	DEGs
Upregulated	*Lilrb4, Plek, Slc7a8, Galk1, St3gal4, Myrf, Mmp12, Cyp3a23/3a1, Psca, Tnc, Pmf1, Gar1, Il17b, Soat1, Hmox1, Tes, Gpnmb, Tmem229b, Ripk1, RGD1561778, Basp1, Cd53, Lyl1, Gpsm3, RGD1564450, Tubb6, Ctsz, Kctd3, Clec4a3, Cotl1, Casp8, Sdc1, Ttc9, Cd14, Mmp14, Tyrobp, Anpep, Fgf7, Knstrn, Ctss, Sppl2b, LOC100910669, Mpeg1, Sat1, Srpx2, Spint2, Plcb3, Kif26b, Fxyd2, Ccl6, Postn, Arl11, Pld3, Man2a1, Vat1, MGC112715, Sfrp2, Col1a1, Igsf6, Cdh11*
Downregulated	*Tuba8, Cds1, Acsl6, Fabp1, Baz2b, Pth2r, Kcnj12, Zfand4, Elmod1, Mcpt2*

Abbreviations: DEG, differentially expressed gene; IR, ischemia/reperfusion; SH, sham.

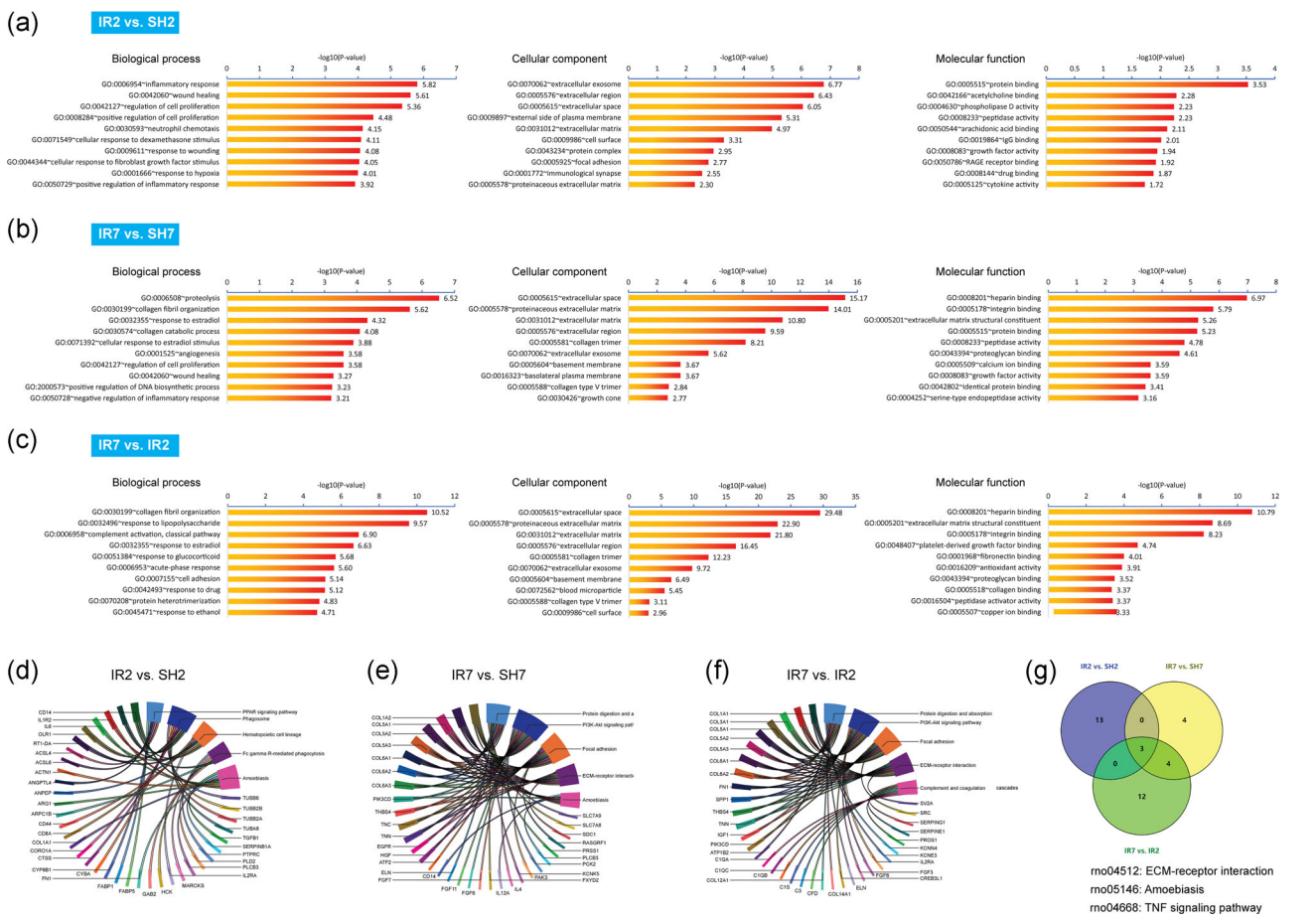

FIGURE 3 GO and KEGG analyses of DEGs. (a–c) Top 10 enriched biological process, molecular function, and cellular component terms for IR2 versus SH2, IR7 versus SH7, and IR7 versus IR2, respectively. (d–f) Chord plots showing the relationship between DEGs and the top five enriched KEGG pathways for three comparisons, respectively. (g) Venn's diagram showing common KEGG pathways. DEG, differentially expressed gene; GO, gene ontology; IR, ischemia/reperfusion; KEGG, Kyoto encyclopedia of genes and genomes; SH, sham

with node degree ≥ 10 were found, with the top 10 hub proteins encoded by *Ctss*, *Tyrobp*, *Mmp12*, *Plek*, *Cd53*, *Col1a1*, *Clec4a3*, *Lilrb4*, *Anpep*, and *Ccl6* (Figure 4b). By using the MCODE, several key modules were identified, with the Module 1 (in yellow) containing the most highly clustered proteins (Figure 4c). These proteins are encoded by *Ctss*, *Ctsz*, *LOC685020*, *Spint2*, *Fgf7*, *Mmp14*, *Arl11*, *Igsf6*, *Cdh11*, *Gpnmb*, *Mpeg1*, *Plek*, *Clec4a3*, *Sdc1*, *Col1a1*, *Postn*, *Gpsm3*, *Ccl6*, *Cd53*, *RGD1561778*, *Anpep*, *Lilrb4*, *Cd14*, *Tyrobp*, and *Casp8* (Figure 4d). The other two modules consisted of only a few proteins (Figure 4e).

3.4 | Identification of three key genes

On the basis of 25 genes encoding the highly clustered proteins in Module 1, GO and KEGG enrichment analyses were performed. The top three significantly enriched BP categories included extracellular structure organization, response to TNF, and cell differentiation (Figure 5a). The enriched MF and CC categories are shown in Figure 5b,c. Of note, the enrichment in the response to TNF was in line with the findings of the inflammatory response in Figure 3a and TNF signaling pathway in Figure 3g. KEGG analysis highlighted the apoptosis signaling pathway, involving three key genes: *Ctss*, *Ctsz*, and *Casp8* (Figure 5d).

On the basis of bioinformatic analysis of the gene expression profile underlying myocardial I/R injury, *Ctss*, *Ctsz*, and *Casp8* were identified in relation to the TNF signaling pathway (Figure 5e) and apoptosis pathway (Figure 5f).

3.5 | Validation of three key genes

After revealing three key genes during myocardial I/R injury, we searched the GEO database to validate their expression in other myocardial I/R injury datasets. First, in GSE61592, mice underwent 90 min of left anterior descending coronary artery occlusion followed by reperfusion for 3 days or 72 hr, which is similar to the conditions in this study. Next, we investigated whether the changes of these genes were still significant in the long-term following myocardial I/R. In GSE22489, rats underwent myocardial ischemia followed by

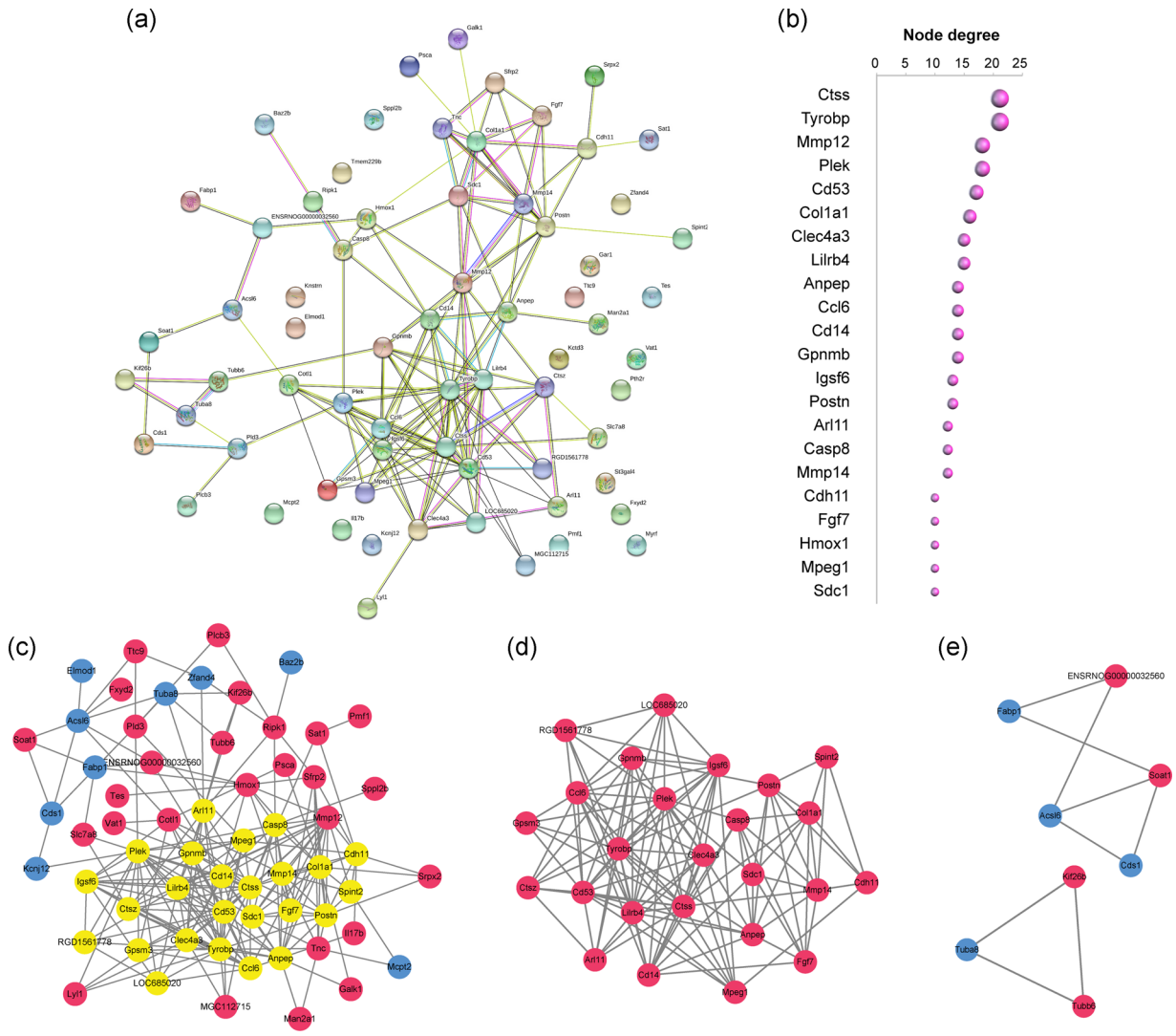

FIGURE 4 PPI analysis of common DEGs. (a) Interaction network of proteins encoded by the 70 common DEGs. (b) The top 10 hub proteins with high node degree. (c) MCODE networks showing several key modules. (d) Module 1 containing 25 highly clustered proteins. (e) Modules 2 and 3 with a few proteins. DEG, differentially expressed gene; MCODE, molecular complex detection; PPI, protein–protein interaction

reperfusion for 4 weeks, representing a situation of chronic I/R-induced myocardial injury. Thereafter, we assessed the expression of these key genes in a human dataset GSE97320.

In GSE61592, myocardial I/R-induced significant activation of ctss, ctsz, and casp8 in mouse myocardium at 72 hr of reperfusion (Figure 6a). In GSE22489, myocardial I/R rats showed significantly increased levels of ctss and ctsz, but not casp8, at 4 weeks of reperfusion (Figure 6b). In GSE97320, patients with MI had elevated expression of the three genes in their peripheral blood, in which the ctss level showed a more than 100 times increase compared to the healthy controls (Figure 6c).

Furthermore, the myocardial I/R (ischemia for 30 min and reperfusion for 24 hr) induced significantly increased protein expression of cathepsin S (encoded by *Ctss*), cathepsin Z (*Ctsz*), caspase-8 (*Casp8*), and cleaved caspase-8 in the left ventricle tissues of mice (Figure 6e,f).

3.6 | Inhibition of cathepsin S attenuated myocardial I/R-induced injury by suppressing inflammation and apoptosis

The PPI analysis revealed that cathepsin S was the top hub protein with the highest connectivity, thus the role of cathepsin S was further investigated in I/R-induced myocardial injury in mice. Compared to the SH mice, myocardial I/R induced remarkable increases in the protein expression of cleaved caspase-8, cleaved caspase-3, and cleaved PARP. These changes were effectively blocked by the use of two different selective cathepsin S inhibitors, LY3000328 and MIV-247 (Figure 7a).

To evaluate the myocardial injury, serum cTnI, LDH, and CK-MB levels in the SH and myocardial I/R mice were tested. Myocardial I/R led to elevated serum cTnI, LDH, and CK-MB levels, while the

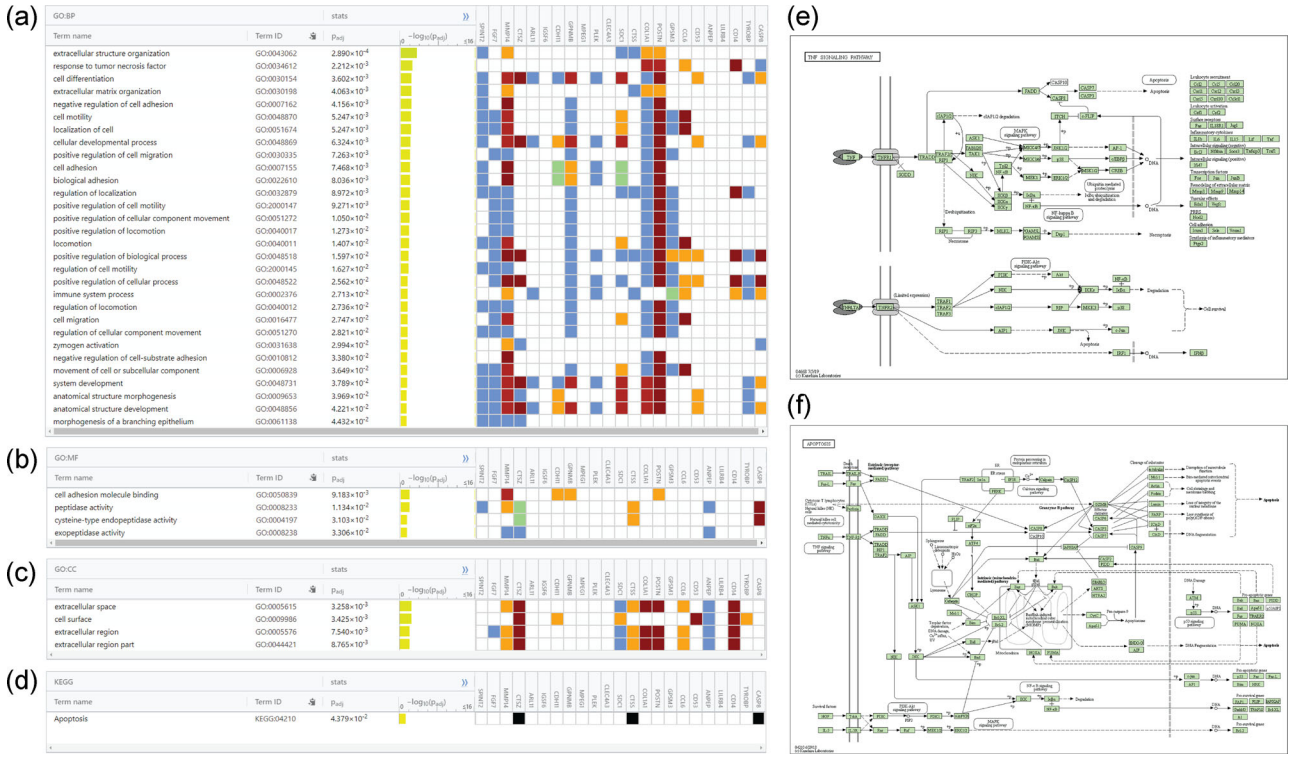

FIGURE 5 Identification of three key genes. (a–c) Significantly enriched BP, MF, and CC terms of the 25 genes. (d) Enriched apoptosis pathway in KEGG analysis. (e) TNF signaling pathway. (f) Apoptosis pathway. BP, biological process; CC, cellular component; KEGG, Kyoto encyclopedia of genes and genomes; MF, molecular function; TNF, tumor necrosis factor

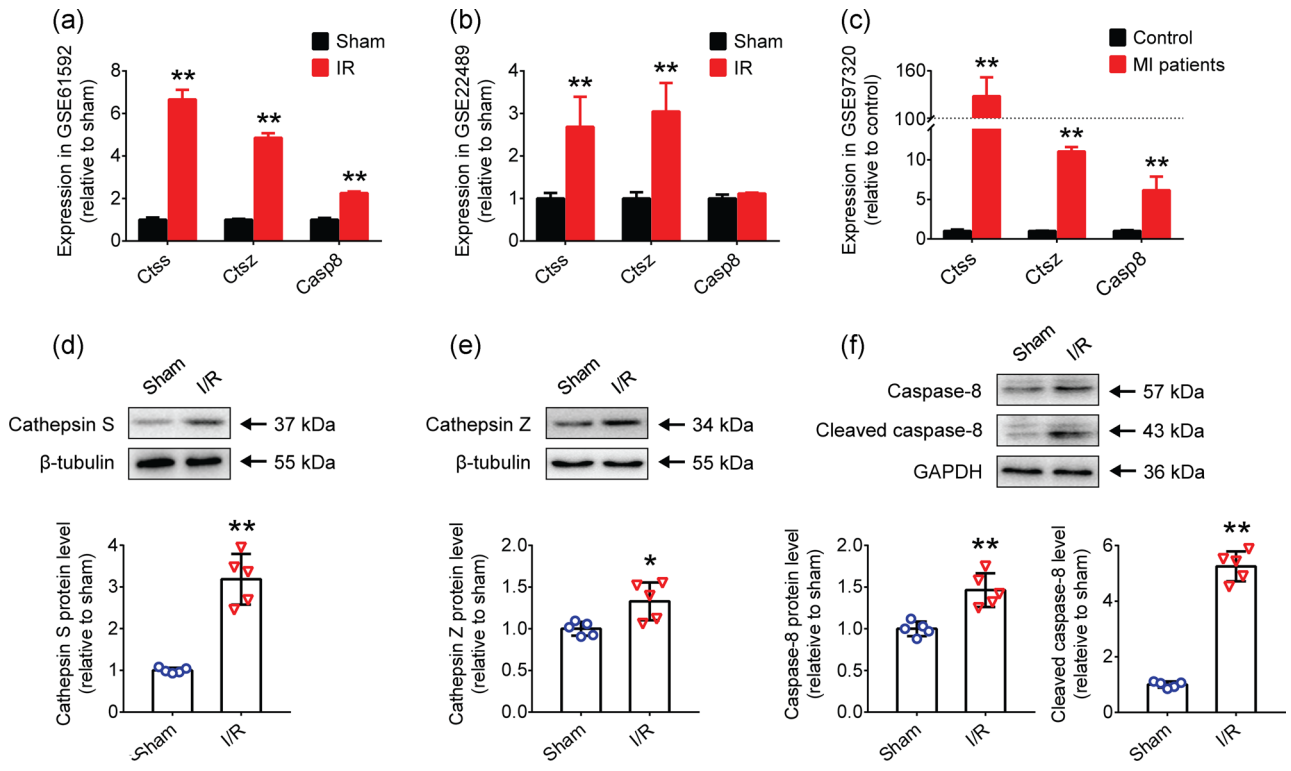

FIGURE 6 Validation of three key genes. (a,b) Validation in two murine datasets (GSE61592 and GSE22489). (c) Validation in a human dataset (GSE97320). (d–f) Protein expression of cathepsin S, cathepsin Z, caspase-8, and cleaved caspase-8 in the left ventricle tissues of mice during myocardial I/R injury. (a–c) $n = 3$, (d–f) $n = 5$. $^{*}p < .05$, $^{**}p < .01$ versus the control or sham group. GAPDH, glyceraldehyde 3-phosphate dehydrogenase; I/R, ischemia/reperfusion; MI, myocardial infarction

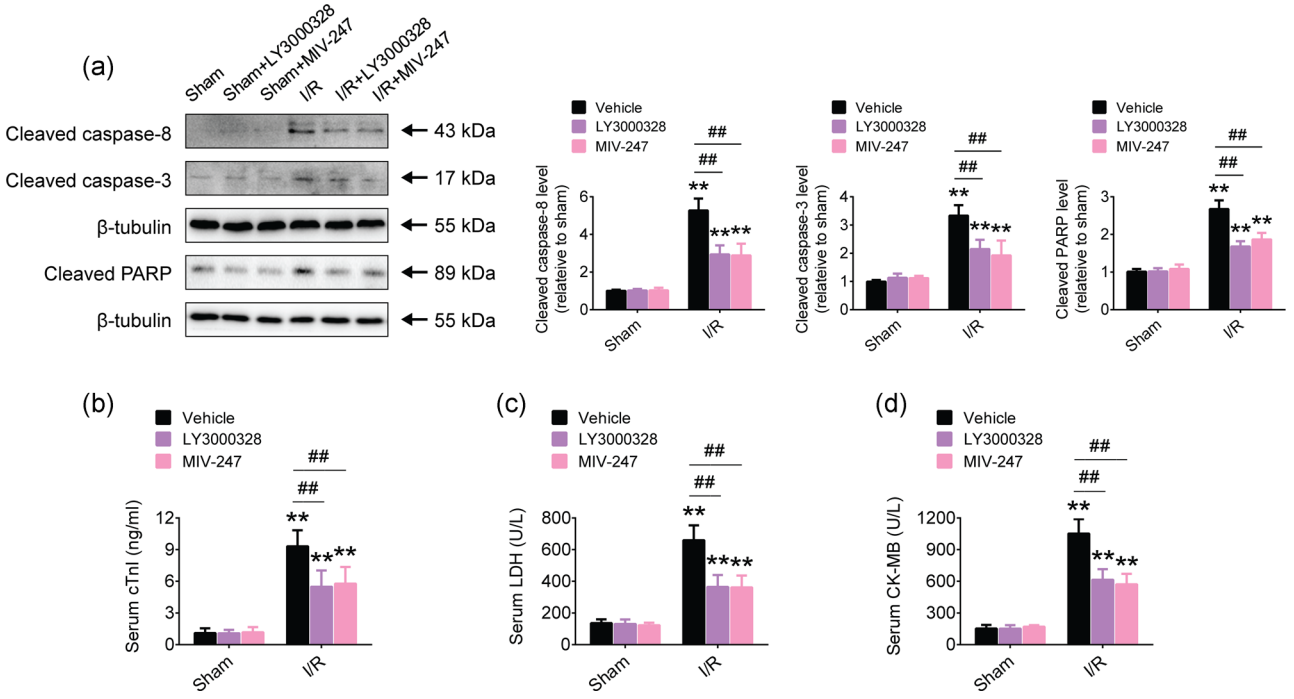

FIGURE 7 Effects of cathepsin S inhibition on the expression of apoptosis-related proteins and I/R-induced myocardial injury. (a) Western blots showing protein expression of cleaved caspase-8, cleaved caspase-3, and cleaved PARP in the myocardium of sham and myocardial I/R mice. (b–d) LY3000328 or MIV-247 inhibited I/R-induced serum cTnI, LDH, and CK-MB levels. $n = 5$. $^{**}p < .01$ versus the sham group; $^{\#\#}p < .01$ for the comparisons shown. CK-MB, creatinine kinase-MB; cTnI, cardiac troponin I; I/R, ischemia/reperfusion; LDH, lactic dehydrogenase; PARP, poly ADP-ribose polymerase

inhibition of cathepsin S significantly reduced these myocardial injury biomarkers (Figure 7b–d).

To assess myocardial inflammation and apoptosis, the levels of IL-1β, IL-6, and TNF-α in the myocardium and TUNEL apoptosis rate were determined. Myocardial I/R resulted in a significantly increased apoptosis rate (Figure 8a) and expression of inflammatory cytokines (Figure 8b–d), which was reversed by cathepsin S inhibition.

Finally, the effects of cathepsin S inhibition on myocardial I/R-induced mortality at 21 days of reperfusion in mice were investigated. Kaplan–Meier survival analysis demonstrated that the inhibition of cathepsin S improved 21-day survival following myocardial I/R injury, with the survival rate of 15/18 (83.3%) for LY3000328 and 17/19 (89.5%) for MIV-247, compared to 10/20 (50%) in the I/R mice (Figure 8e).

4 | DISCUSSION

In this study, the gene expression profile during myocardial I/R injury was analyzed to identify a number of DEGs in three subgroups: 353 in IR2 versus SH2, 447 in IR7 versus SH7, and 340 in IR7 versus IR2. GO and KEGG analyses of the DEGs indicated significantly enriched BP of the inflammatory response and TNF signaling pathway. On the basis of common DEGs, PPI network and MCODE assay revealed 25 hub proteins in the most highly clustered module. Further functional analyses highlighted three key genes (*Ctss*, *Ctsz*, and *Casp8*) associated with TNF and apoptosis pathways. Next, the messenger RNA expression of the three genes was validated in two murine datasets and one human dataset, and the protein expression was confirmed in myocardial I/R mice. In the functional experiments in mice, myocardial I/R led to significant increases in the levels of myocardial injury biomarkers, inflammatory cytokines, and apoptosis rate, as well as activation of apoptosis-related proteins including cleaved caspase-8, cleaved caspase-3, and cleaved PARP, while inhibition of cathepsin S (encoded by *Ctss*) alleviated these changes and improved survival rate following myocardial I/R injury.

In a previous study, Roy et al. (2006) showed gene changes related to inflammation and extracellular matrix in the early and late phases of I/R heart. They found activation of IL-6, IL-18, and caspase-2, caspase-3, and caspase-8 in response to myocardial I/R. Our study is distinct from the previous one by the discovery of two novel candidate genes, *Ctss* and *Ctsz*. We then used three different myocardial I/R datasets for validation. Next, we established the mouse myocardial I/R injury model and showed significantly elevated protein expression of cathepsin S, cathepsin Z, caspase-8, and cleaved caspase-8. These key genes were associated with BPs and signaling pathways of inflammation and apoptosis. Moreover, we found that cathepsin S inhibition by two different selective cathepsin S inhibitors, LY3000328 or MIV-247, alleviated myocardial I/R-induced injury by suppressing inflammation and apoptosis.

TNF is a critical cytokine that induces a wide range of intracellular signal pathways including cell survival, immunity,

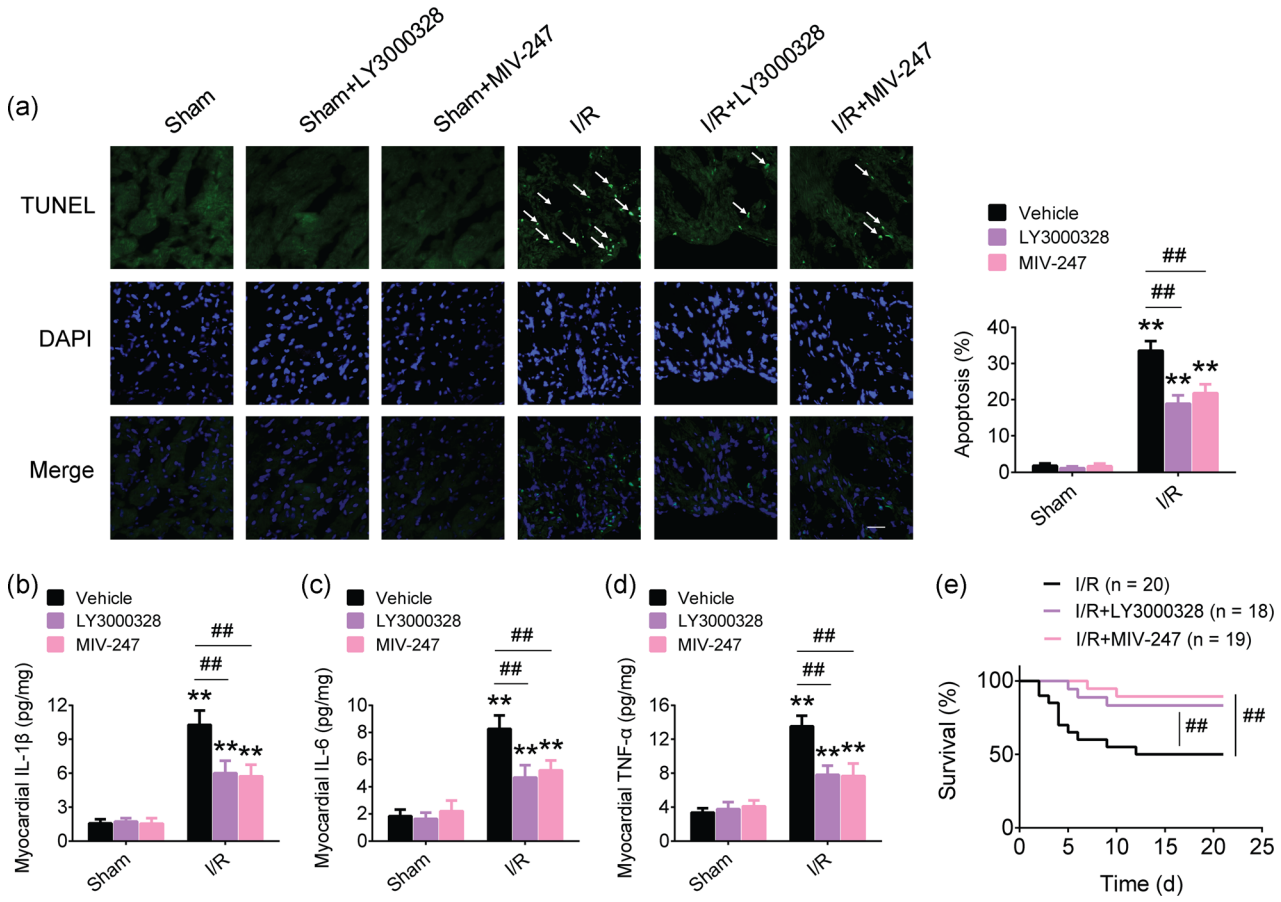

FIGURE 8 Effects of cathepsin S inhibition on apoptosis, inflammation, and survival following I/R-induced myocardial injury. (a) LY3000328 or MIV-247 reduced I/R-induced TUNEL apoptosis in the myocardium of mice. (b–d) LY3000328 or MIV-247 blocked myocardial I/R-induced IL-1β, IL-6, and TNF-α expression. (e) Kaplan–Meier plot showing inhibition of cathepsin S improved survival following myocardial I/R. Scale bar = 50 μm. $n = 5$ (a–d). $^{**}p < .01$ versus the sham group; $^{\#\#}p < 0.01$ for the comparisons shown. DAPI, 4′,6-diamidino-2-phenylindole; IL-1β, interleukin-1β; IL-6, interleukin-6; I/R, ischemia/reperfusion; TNF-α, tumor necrosis factor-α; TUNEL, TdT-mediated dUTP nick-end labeling

apoptosis, and inflammation (Ting & Bertrand, 2016; Wallach, 2016). Inflammation associated with the TNF signaling pathway is critical during myocardial I/R as well as in the pathology of a wide range of diseases (Shao et al., 2019; Song et al., 2020; Williams, Huang, & Randolph, 2019; Yang et al., 2020). Suppressing inflammation by targeting the transcription factor nuclear factor-κB helps us to prevent MI and other diseases including colitis, cystic fibrosis, arthritis, and atopic dermatitis (Giridharan & Srinivasan, 2018). Caspase-8, a caspase protein encoded by the *Casp8* gene, plays an essential role in cell apoptosis induced by death receptors including the TNF receptors, Fas/Apo1, and DR3 (Varfolomeev et al., 1998). Jin, Shi, Liu, Chen, and Yang (2019) showed that a new type of xanthones promoted HepG2 cell apoptosis through enhancing the expression of cleaved caspase-8, caspase-9, and caspase-3. Qiu et al. (2019) also found that apigenin inhibited cell proliferation and induced cell apoptosis by activating the caspase-8 expression. Besides the proapoptosis function, recent studies showed the prosurvival effects of caspase-8. Newton, Wickliffe, Maltzman et al. (2019) recently showed that caspase-8 protected against necroptosis and determined plasticity between cell death pathways. Another study also demonstrated that the cleavage of receptor-interacting serine/threonine-protein kinase 1 by caspase-8 played an essential role in limiting apoptosis and necroptosis (Newton, Wickliffe, Dugger et al., 2019). Therefore, caspase-8 exerts both prodeath and prosurvival effects in different circumstances.

To date, the roles of *Ctss* and *Ctsz* in myocardial I/R injury remain unclear. Cathepsin S and cathepsin Z are two lysosomal proteases of the cathepsin family. Cathepsins play an essential role in various pathological conditions including heart valve disease, cardiomyopathy, cardiovascular repair, atherosclerosis, and autoimmune disease (Sena, Figueiredo, & Aikawa, 2017). Of the 11 members of cathepsins in humans, cathepsin S is a particularly potent one that contributes to enhanced cardiovascular inflammation and calcification (Sena et al., 2017). In a cohort study of elderly men, a high level of cathepsin S was associated with high serum inflammatory markers in the 7-year follow-up (Jobs et al., 2010). H. Chen et al. (2013) found that MI mice had increased level and activity of cathepsin S which was associated with left ventricular remodeling. During neuropathic pain in mice, the inhibition of cathepsin S alleviated mechanical allodynia and improved the effects of gabapentin and pregabalin

(Hewitt et al., 2016). In lupus nephritis, cathepsin S blockade suppressed systemic and peripheral autoimmune tissue injury (Tato et al., 2017). In a mouse cardiac transplantation model, inhibiting cathepsin S and calcineurin suppressed donor-specific antibody production (Kubo et al., 2018). For cathepsin Z, a study showed that cathepsin Z deficiency reduced IL-1β-driven neuroinflammation in mice (Allan et al., 2017).

According to our pilot experiments, most of the deaths occurred within 10 days following myocardial I/R injury. To evaluate the effects of cathepsin S inhibition on the long-term outcomes of mice after myocardial I/R, we lengthened the observation period to 21 days or 3 weeks, which is approximately equivalent to two human years. Through the Kaplan–Meier survival analysis, we found that cathepsin S inhibition improved survival rates of mice up to 21 days after myocardial I/R injury.

The first limitation of this study is that the functional enrichment results of DEGs were based on gene expression profiles in a previous database and the sample size was relatively small. Second, the expression was only on the gene level, without data on the noncoding RNAs or the interactions. Third, this study showed that the inhibition of cathepsin S protein expression attenuated myocardial I/R injury in mice. To get a more comprehensive understanding of the mechanisms, further investigations are required to explore the impact of cathepsin S overexpression on cardiomyocytes under normal conditions and during myocardial I/R injury. Finally, the roles of the other two key candidate genes (*Ctsz* and *Casp8*) in myocardial I/R injury need to be assessed in future studies.

In conclusion, this study revealed three key candidate genes (*Ctss*, *Ctsz*, and *Casp8*) related to inflammation and apoptosis pathways during myocardial I/R injury, and their expressions were validated on several gene expression profile datasets and in myocardial I/R mice. Further functional experiments suggest that the inhibition of cathepsin S (encoded by *Ctss*) alleviated myocardial I/R-induced injury in mice by suppressing inflammation and apoptosis. On the basis of these findings, cathepsin S inhibition may be useful for cardioprotection in the clinical settings.

ACKNOWLEDGMENTS

This study was supported by the National Natural Science Foundation of China (81873925 and 81671880 to Fu-Hai Ji, 81701098 to Xiao-Wen Meng, and 81601659 to Ke Peng), Jiangsu Provincial Medical Youth Talents Program (QNRC2016741 to Ke Peng), Jiangsu Government Scholarship for Overseas Studies (JS-2018-178 to Ke Peng), Jiangsu Provincial Medical Innovation Team (CXTDA2017043 to Fu-Hai Ji), and Suzhou Key Disease Program (LCZX201603 to Fu-Hai Ji).

CONFLICT OF INTERESTS

The authors declare that there are no conflict of interests.

AUTHOR CONTRIBUTIONS

K. P., F.-H. J., and Z. X. contributed to the conception and design of the study. K. P. drafted the manuscript. K. P., X.-W. M., and S.-Y. S. conducted the study and analyzed the data. H. L. and B. Y. contributed to the review and revision of the manuscript. All authors read and approved the final manuscript.

DATA AVAILABILITY STATEMENT

The data that support the findings of this study are available in GEO at https://www.ncbi.nlm.nih.gov/geo/ and in the Supporting Information of this article.

ORCID

Ke Peng http://orcid.org/0000-0003-2879-1759
Fu-Hai Ji http://orcid.org/0000-0001-6649-665X

REFERENCES

Allan, E. R. O., Campden, R. I., Ewanchuk, B. W., Tailor, P., Balce, D. R., McKenna, N. T., … Yates, R. M. (2017). A role for cathepsin Z in neuroinflammation provides mechanistic support for an epigenetic risk factor in multiple sclerosis. *Journal of Neuroinflammation*, *14*(1), 103.

Bader, G. D., & Hogue, C. W. (2003). An automated method for finding molecular complexes in large protein interaction networks. *BMC Bioinformatics*, *4*, 2.

Chen, J., Jiang, Z., Zhou, X., Sun, X., Cao, J., Liu, Y., & Wang, X. (2019). Dexmedetomidine preconditioning protects cardiomyocytes against hypoxia/reoxygenation-induced necroptosis by inhibiting HMGB1-mediated inflammation. *Cardiocasular Drugs and Therapy*, *33*(1), 45–54.

Chen, H., Wang, J., Xiang, M. X., Lin, Y., He, A., Jin, C. N., … Shi, G. P. (2013). Cathepsin S-mediated fibroblast trans-differentiation contributes to left ventricular remodelling after myocardial infarction. *Cardiovascular Research*, *100*(1), 84–94.

Chi, H. J., Chen, M. L., Yang, X. C., Lin, X. M., Sun, H., Zhao, W. S., … Cai, J. (2017). Progress in therapies for myocardial ischemia reperfusion injury. *Current Drug Targets*, *18*(15), 1712–1721.

Davidson, S. M., Ferdinandy, P., Andreadou, I., Botker, H. E., Heusch, G., Ibanez, B., … Action, C. C. (2019). Multitarget strategies to reduce myocardial ischemia/reperfusion injury: JACC review topic of the week. *Journal of the American College of Cardiology*, *73*(1), 89–99.

Giridharan, S., & Srinivasan, M. (2018). Mechanisms of NF-κB p65 and strategies for therapeutic manipulation. *Journal of Inflammation Research*, *11*, 407–419.

Hausenloy, D. J., & Yellon, D. M. (2013). Myocardial ischemia-reperfusion injury: A neglected therapeutic target. *Journal of Clinical Investigation*, *123*(1), 92–100.

Hewitt, E., Pitcher, T., Rizoska, B., Tunblad, K., Henderson, I., Sahlberg, B. L., … Lindstrom, E. (2016). Selective cathepsin S inhibition with MIV-247 attenuates mechanical allodynia and enhances the antiallodynic effects of gabapentin and pregabalin in a mouse model of neuropathic pain. *Journal of Pharmacology and Experimental Therapeutics*, *358*(3), 387–396.

Jadhav, P. K., Schiffler, M. A., Gavardinas, K., Kim, E. J., Matthews, D. P., Staszak, M. A., … Deng, G. G. (2014). Discovery of cathepsin S inhibitor LY3000328 for the treatment of abdominal aortic aneurysm. *ACS Medicinal Chemistry Letters*, *5*(10), 1138–1142.

Jiao, X., Sherman, B. T., Huang da, W., Stephens, R., Baseler, M. W., Lane, H. C., & Lempicki, R. A. (2012). DAVID-WS: A stateful web service to facilitate gene/protein list analysis. *Bioinformatics*, *28*(13), 1805–1806.

Jin, S., Shi, K., Liu, L., Chen, Y., & Yang, G. (2019). Xanthones from the bark of *Garcinia xanthochymus* and the mechanism of induced apoptosis in human hepatocellular carcinoma HepG2 cells via the mitochondrial pathway. *International Journal of Molecular Sciences*, *20*(19), 4803.

Jobs, E., Riserus, U., Ingelsson, E., Helmersson, J., Nerpin, E., Jobs, M., … Arnlov, J. (2010). Serum cathepsin S is associated with serum C-reactive protein and interleukin-6 independently of obesity in elderly men. *Journal of Clinical Endocrinology and Metabolism*, *95*(9), 4460–4464.

Kubo, K., Kawato, Y., Nakamura, K., Nakajima, Y., Nakagawa, T. Y., Hanaoka, K., … Higashi, Y. (2018). Effective suppression of donor specific antibody production by Cathepsin S inhibitors in a mouse transplantation model. *European Journal of Pharmacology*, *838*, 145–152.

Lei, S., Su, W., Xia, Z. Y., Wang, Y., Zhou, L., Qiao, S., … Irwin, M. G. (2019). Hyperglycemia-induced oxidative stress abrogates remifentanil preconditioning-mediated cardioprotection in diabetic rats by impairing caveolin-3-modulated PI3K/Akt and JAK2/STAT3 signaling. *Oxidative Medicine and Cellular Longevity*, *2019*, 9836302.

Newton, K., Wickliffe, K. E., Dugger, D. L., Maltzman, A., Roose-Girma, M., Dohse, M., … Dixit, V. M. (2019). Cleavage of RIPK1 by caspase-8 is crucial for limiting apoptosis and necroptosis. *Nature*, *574*(7778), 428–431.

Newton, K., Wickliffe, K. E., Maltzman, A., Dugger, D. L., Reja, R., Zhang, Y., … Dixit, V. M. (2019). Activity of caspase-8 determines plasticity between cell death pathways. *Nature*, *575*(7784), 679–682.

Peng, K., Chen, W. R., Xia, F., Liu, H., Meng, X. W., Zhang, J., … Ji, F. H. (2020). Dexmedetomidine post-treatment attenuates cardiac ischaemia/reperfusion injury by inhibiting apoptosis through HIF-1alpha signalling. *Journal of Cellular and Molecular Medicine*, *24*(1), 850–861.

Qiu, J. G., Wang, L., Liu, W. J., Wang, J. F., Zhao, E. J., Zhou, F. M., … Jiang, B. H. (2019). Apigenin inhibits IL-6 transcription and suppresses esophageal carcinogenesis. *Frontiers in Pharmacology*, *10*, 1002.

Raudvere, U., Kolberg, L., Kuzmin, I., Arak, T., Adler, P., Peterson, H., & Vilo, J. (2019). g:Profiler: A web server for functional enrichment analysis and conversions of gene lists (2019 update). *Nucleic Acids Research*, *47*(W1), W191–W198.

Ritchie, M. E., Phipson, B., Wu, D., Hu, Y., Law, C. W., Shi, W., & Smyth, G. K. (2015). limma powers differential expression analyses for RNA-sequencing and microarray studies. *Nucleic Acids Research*, *43*(7), e47.

Roy, S., Khanna, S., Kuhn, D. E., Rink, C., Williams, W. T., Zweier, J. L., & Sen, C. K. (2006). Transcriptome analysis of the ischemia-reperfused remodeling myocardium: Temporal changes in inflammation and extracellular matrix. *Physiological Genomics*, *25*(3), 364–374.

Sena, B. F., Figueiredo, J. L., & Aikawa, E. (2017). Cathepsin S as an inhibitor of cardiovascular inflammation and calcification in chronic kidney disease. *Frontiers in Cardiovascular Medicine*, *4*, 88.

Shannon, P., Markiel, A., Ozier, O., Baliga, N. S., Wang, J. T., Ramage, D., … Ideker, T. (2003). Cytoscape: A software environment for integrated models of biomolecular interaction networks. *Genome Research*, *13*(11), 2498–2504.

Shao, P., Guo, N., Wang, C., Zhao, M., Yi, L., Liu, C., … Shen, H. (2019). Aflatoxin G1 induced TNF-alpha-dependent lung inflammation to enhance DNA damage in alveolar epithelial cells. *Journal of Cellular Physiology*, *234*(6), 9194–9206.

Song, Y. F., Zhao, L., Wang, B. C., Sun, J. J., Hu, J. L., Zhu, X. L., … Ge, Z. W. (2020). The circular RNA TLK1 exacerbates myocardial ischemia/reperfusion injury via targeting miR-214/RIPK1 through TNF signaling pathway. *Free Radical Biology and Medicine*, *155*, 69–80.

Steimle, A., Gronbach, K., Beifuss, B., Schafer, A., Harmening, R., Bender, A., … Frick, J. S. (2016). Symbiotic gut commensal bacteria act as host cathepsin S activity regulators. *Journal of Autoimmunity*, *75*, 82–95.

Szklarczyk, D., Gable, A. L., Lyon, D., Junge, A., Wyder, S., Huerta-Cepas, J., … Mering, C. V. (2019). STRING v11: Protein-protein association networks with increased coverage, supporting functional discovery in genome-wide experimental datasets. *Nucleic Acids Research*, *47*, D607–D613.

Tato, M., Kumar, S. V., Liu, Y., Mulay, S. R., Moll, S., Popper, B., … Anders, H. J. (2017). Cathepsin S inhibition combines control of systemic and peripheral pathomechanisms of autoimmune tissue injury. *Scientific Reports*, *7*(1), 2775.

Ting, A. T., & Bertrand, M. J. M. (2016). More to Life than NF-κB in TNFR1 Signaling. *Trends in Immunology*, *37*(8), 535–545.

Toldo, S., Mauro, A. G., Cutter, Z., & Abbate, A. (2018). Inflammasome, pyroptosis, and cytokines in myocardial ischemia-reperfusion injury. *American Journal of Physiology: Heart and Circulatory Physiology*, *315*(6), H1553–H1568.

Varfolomeev, E. E., Schuchmann, M., Luria, V., Chiannilkulchai, N., Beckmann, J. S., Mett, I. L., … Wallach, D. (1998). Targeted disruption of the mouse Caspase 8 gene ablates cell death induction by the TNF receptors, Fas/Apo1, and DR3 and is lethal prenatally. *Immunity*, *9*(2), 267–276.

Wallach, D. (2016). The cybernetics of TNF: Old views and newer ones. *Seminars in Cell & Developmental Biology*, *50*, 105–114.

Wang, T. T., Shi, M. M., Liao, X. L., Li, Y. Q., Yuan, H. X., Li, Y., … Ou, J. S. (2019). Overexpression of inducible nitric oxide synthase in the diabetic heart compromises ischemic postconditioning. *Journal of Molecular and Cellular Cardiology*, *129*, 144–153.

Wang, S., Wang, C., Yan, F., Wang, T., He, Y., Li, H., … Zhang, Z. (2017). N-acetylcysteine attenuates diabetic myocardial ischemia reperfusion injury through inhibiting excessive autophagy. *Mediators of Inflammation*, *2017*, 9257291.

Williams, J. W., Huang, L. H., & Randolph, G. J. (2019). Cytokine circuits in cardiovascular disease. *Immunity*, *50*(4), 941–954.

Xia, Z., Li, H., & Irwin, M. G. (2016). Myocardial ischaemia reperfusion injury: The challenge of translating ischaemic and anaesthetic protection from animal models to humans. *British Journal of Anaesthesia*, *117*(Suppl. 2), ii44–ii62.

Yang, B., Sun, H., Xu, X., Zhong, H., Wu, Y., & Wang, J. (2020). YAP1 inhibits the induction of TNF-alpha-stimulated bone-resorbing mediators by suppressing the NF-kappaB signaling pathway in MC3T3-E1 cells. *Journal of Cellular Physiology*, *235*(5), 4698–4708.

Yuan, M., Meng, X. W., Ma, J., Liu, H., Song, S. Y., Chen, Q. C., … Peng, K. (2019). Dexmedetomidine protects H9c2 cardiomyocytes against oxygen-glucose deprivation/reoxygenation-induced intracellular calcium overload and apoptosis through regulating FKBP12.6/RyR2 signaling. *Drug Design, Development and Therapy*, *13*, 3137–3149.

Zhang, J. J., Peng, K., Zhang, J., Meng, X. W., & Ji, F. H. (2017). Dexmedetomidine preconditioning may attenuate myocardial ischemia/reperfusion injury by down-regulating the HMGB1-TLR4-MyD88-NF-κB signaling pathway. *PLoS One*, *12*(2), e0172006.

Zhang, T., Zhang, Y., Cui, M., Jin, L., Wang, Y., Lv, F., … Xiao, R. P. (2016). CaMKII is a RIP3 substrate mediating ischemia- and oxidative stress-induced myocardial necroptosis. *Nature Medicine*, *22*(2), 175–182.

How to cite this article: Peng K, Liu H, Yan B, et al. Inhibition of cathepsin S attenuates myocardial ischemia/reperfusion injury by suppressing inflammation and apoptosis. *J Cell Physiol*. 2020;1–12. https://doi.org/10.1002/jcp.29938